Neutrino induced pion production at MiniBooNE and K2K energies

T. Leitner*, O. Buss*, U. Mosel* and L. Alvarez-Ruso†

*Institut für Theoretische Physik, Universität Giessen, Germany
†Departamento de Física, Centro de Física Computacional, Universidade de Coimbra, Portugal

Abstract. We investigate charged and neutral current neutrino-induced incoherent pion production off nuclei within the GiBUU model at energies relevant for the MiniBooNE and K2K experiments. Special attention is paid to the entanglement between measured CCQE and CC1π^+ cross sections. We further give predictions and compare to recent data measured at MiniBooNE.

Keywords: neutrino-nucleus interactions, pion production, quasielastic scattering
PACS: 13.15.+g, 25.30.Pt

INTRODUCTION

A proper understanding of neutrino induced pion production is essential for the interpretation of current neutrino oscillations experiments. A good knowledge of the neutrino energy is required for a precise determination of oscillation parameters in ν_μ disappearance measurements. These experiments search for a distortion in the neutrino flux at the detector positioned far away from the source. By comparing both, near and far neutrino energy spectra, one gains information about the oscillation probability and with that about mixing angles and mass squared differences. However, the neutrino energy is not measurable directly but has to be reconstructed from the reaction products. Present oscillation experiments use the CCQE reaction both as signal event and to reconstruct the neutrino energy from the outgoing muon with two-body kinematics assuming the target nucleon is at rest. CCQE is defined as $\nu_\ell n \to \ell^- p$ on a single nucleon; in the nucleus, CCQE is masked by final-state interactions (FSI). Thus, the correct identification of CCQE events is directly related to the question of how FSI influence the event selection. The main background to CCQE is CC1π^+ production. If the pion is absorbed in the nucleus and/or not seen in the detector, these events can be misidentified as CCQE. Consequently, a proper understanding of CCQE *and* CC1π^+ is essential for the reconstruction of the neutrino energy.

The main task in a ν_e appearance experiment like MiniBooNE is to detect electron neutrinos in a (almost) pure ν_μ beam. The signal event, the ν_e CCQE interaction, is dominated by background. A major problem comes from misidentified events, mainly because of the fact, that the MiniBooNE detector cannot distinguish between a photon and an electron. Thus, ν_μ induced neutral current π^0 production, where the π^0 decays into two γs, is the major source of background when one of the photons is not seen or both Cherenkov rings overlap.

As all of the present oscillations experiments use nuclear targets, it is mandatory to consider FSI, i.e., pion rescattering, with and without charge exchange, and absorption in the nuclear medium. A realistic treatment of the FSI can be achieved in the framework of a coupled-channel transport theory — the GiBUU model.

After a brief review of our model, we first discuss the impact of pion production on CCQE measurements. We further investigate the influence of nuclear effects on CC1π^+ and NC1π^0 cross sections, and, where possible, we confront our model to recent data measured at MiniBooNE.

GIBUU MODEL

We treat neutrino-nucleus scattering as a two-step process. In the initial-state step, the neutrinos interact with nucleons embedded in the nuclear medium. In the final-state step, the outgoing particles of the initial reaction are propagated through the nucleus using a hadronic transport approach.

In the energy region relevant for MiniBooNE, SciBooNE and K2K, the elementary νN reaction is dominated by two processes: quasielastic scattering and the excitation of the Δ resonance ($P_{33}(1232)$). Additionally, our model includes

the excitation of 12 N^* and Δ resonances with invariant masses less than 2 GeV and also a non-resonant single-pion background. The nucleon, $N-\Delta$ and $N-N^*$ vector form factors are based on recent electron-scattering data while the axial couplings are obtained assuming PCAC (partial conservation of the axial current). The Q^2 dependence of the nucleon and $N-\Delta$ axial form factors, F_A and C_5^A, is fitted to bubble chamber neutrino-scattering data.

The neutrino-nucleon cross sections are modified in the nuclear medium. Bound nucleons are treated within a local Thomas-Fermi approximation. They are exposed to a mean-field potential which depends on density and momentum. We account for this by evaluating the above cross sections with full in-medium kinematics, i.e., hadronic tensor and phase-space factors are evaluated with in-medium four-vectors. We also take Pauli blocking and collisional broadening of the outgoing hadrons into account. Our model for neutrino-(bound)nucleon scattering is described in detail in Ref. [1].

After the initial neutrino-nucleon interaction, the produced particles propagate out of the nucleus. During propagation they undergo FSI which are simulated with the coupled-channel semi-classical GiBUU transport model (for details, see Ref. [2] and references therein). It is based on the BUU equation which describes the space-time evolution of a many-particle system in a mean-field potential including a collision term. Nucleons and resonances acquire medium-modified spectral functions and are propagated off-shell. Herby we ensure, that vacuum spectral functions are recovered after leaving the nucleus. The collision term accounts for changes (gain and loss) in the phase-space density due to elastic and inelastic collisions between the particles, and also to particle decays into other hadrons. Baryon-meson two-body interactions (e.g., $\pi N \to \pi N$) are described by resonance contributions and a small non-resonant background term; baryon-baryon cross sections (e.g., $NN \to NN$, $RN \to NN$, $RN \to R'N$, $NN \to \pi NN$) are either fitted to data or calculated, e.g., in pion exchange models. The three-body channels $\pi NN \to NN$ and $\Delta NN \to NNN$ are also included. The BUU equations for all particle species are thus coupled through the collision term and also through the potentials. Such a coupled-channel treatment is required to account for side feeding into different channels.

CCQE AND CC$1\pi^+$ ENTANGLEMENT

One challenge is to identify *true* CCQE events in the detector, i.e., muons originating from an initial QE process. To be more precise, true CCQE corresponds to the inclusive CCQE cross section including all medium effects, or, in other words, the CCQE cross section before FSI. The difficulty comes from the fact that the true CCQE events are masked by FSI in a detector built from nuclei. The FSI lead to misidentified events, e.g., an initial Δ whose decay pion is absorbed or which undergoes “pion-less decay” can count as CCQE event — we call this type of background events “fake CCQE” events. We denote every event which looks like a CCQE event by “CCQE-like”.

In general, at Cherenkov detectors such as MiniBooNE CCQE-like events are all those where no pion is detected while in tracking detectors such as K2K-SciBar/SciFi CCQE-like events are those where a single proton track is visible and at the same time no pions are detected.

To investigate the relation between the CCQE-like and true CCQE cross section, we show their ratio as a function of proton and pion momentum thresholds in Fig. 1. As the proton is not at all relevant for the CCQE identification in Cherenkov detectors, the ratio is independent of the proton momentum detection threshold (dashed line in left panel). This is very different in tracking detectors which rely on the detected proton — here the efficiency is reduced to $\approx$10% at a proton momentum threshold of 0.5 GeV (solid line in left panel). Even at $|\vec{p}|^p_{\text{thres}} = 0$ the efficiency does not exceed 80% because of charge-exchange processes that lead to the emission of undetected neutrons and because of secondary proton knockout that leads to multiple-proton tracks. Focussing on the right panel of Fig. 1 we find that the CCQE-like cross section increases for both detector types as $|\vec{p}|^\pi_{\text{thres}}$ increases. In this case even more events with pions in the final state appear as CCQE-like because these pions are below threshold and thus not detected.

Fixing the flux normalization with HARP’s pion-production data, the MiniBooNE collaboration has presented their first, preliminary absolutely normalized total, differential and double differential cross sections for CCQE at this conference and finds an excess of about 35% compared to the total cross section measured at NOMAD, ANL and BNL [3]. We strongly emphasize that these absolute cross sections depend directly on the pion background subtraction which again is based on the Monte Carlo prediction (cf., Ref. [3]).

In Fig. 2, we show our prediction for the double differential cross section at MiniBooNE in muon observables, all calculated with $M_A = 1$ GeV. The left panel shows the true CCQE events. To emphasize the role of “fake” CCQE events, we show the ratio CCQE-like/true CCQE in the right panel. Unlike for monochromatic beams, the QE and Δ peaks are not distinguishable any more but strongly overlap. This fact makes a model-independent cut based on muon variables to subtract the background impossible.

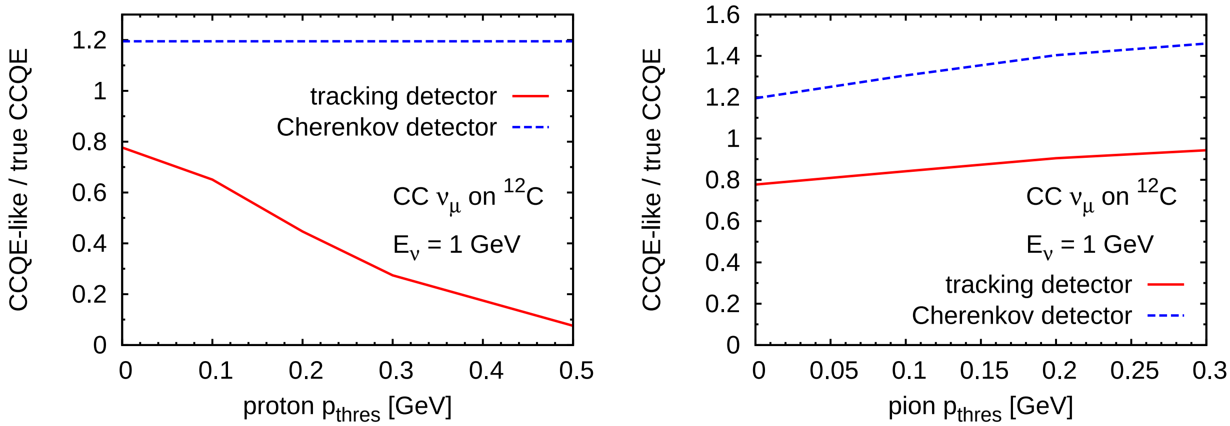

FIGURE 1. Ratio of the CCQE-like to the true CCQE cross section as a function of the proton (pion) momentum detection threshold for CC ν_μ on ^{12}C at $E_\nu = 1$ GeV. The solid lines are obtained using the tracking detector identification, while the dashed lines are for Cherenkov detectors.

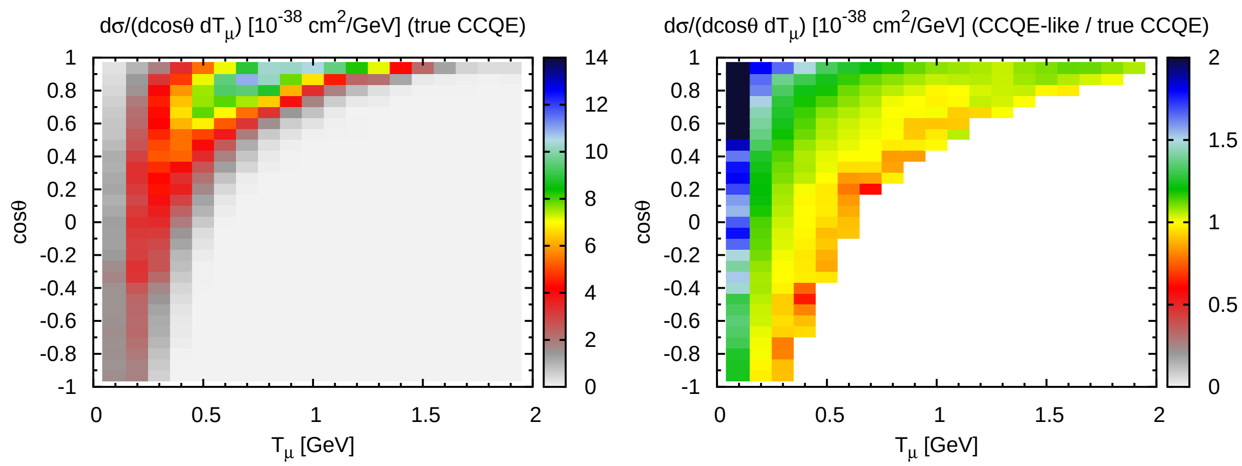

FIGURE 2. Double differential cross section on ^{12}C averaged over the MiniBooNE flux as a function of the muon kinetic energy and the muon scattering angle. The left panel shows the true CCQE cross section, the right panel the ratio of the CCQE-like to the true CCQE cross section.

MINIBOONE'S CC1π^+ MEASUREMENT

In the left panel of Fig. 3 we give our results for the single-π^+/QE ratio for CC interactions on mineral oil CH_2. The solid lines denote the CC1π^+-like/CCQE-like result, the dashed lines stand for the true CC1π^+/true CCQE result, and the dash-dotted lines give the vacuum expectation. Note that we have applied the Cherenkov detector identification criteria.

We emphasize that nuclear corrections cancel out in the ratio, only as long as FSI are not considered ("true" vs. "free"). In general, the complexity of FSI prevent such cancellations as one can infer from the result denoted with "like" which does not coincide with the "true" and "free" ones.

We further compare to very recent MiniBooNE data [4] (Fig. 3 left). Let us first focus on the data denoted with the triangles (upper data set). These are corrected for FSI using a specific Monte Carlo generator, i.e., they give the cross sections for bound nucleons "before FSI". As this procedure introduces a model dependence in the data, a fully consistent comparison is not possible. Ignoring this inconsistency, our calculation denoted with "true" should be the one to compare with. The agreement is perfect for energies up to 1.5 GeV, and still within their error bars for higher E_ν. The MiniBooNE data denoted with bullets (lower data set) is their result for the ratio of CC1π^+-like to CCQE-like.

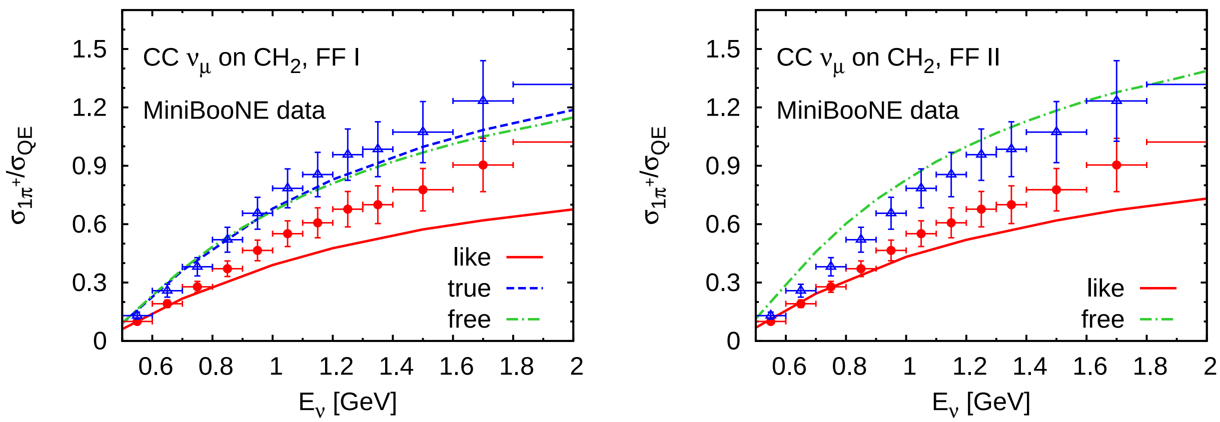

FIGURE 3. Left panel: single-π^+/QE cross section ratio for CC interactions vs. neutrino energy on CH_2 together with recent data from MiniBooNE [4] (upper data set: corrected for FSI, lower data set: uncorrected for FSI). The solid lines denote the CC1π^+-like/CCQE-like result (Cherenkov detector definitions), the dashed lines stand for the true CC1π^+/true CCQE result, and the dash-dotted lines give the vacuum expectation, i.e., the sum of the nucleon cross sections (with two additional protons in the MiniBooNE case). Right panel: same but with a dipole form for C_5^A (see text).

As these data are not corrected for FSI within a specific Monte Carlo event generator, this observable is less model dependent. Still, the energy reconstruction requires specific assumptions as well as the detector simulation. We find that our calculation clearly underestimates the uncorrected data. However, the perfect agreement with their corrected distribution indicates a significant difference between the pion absorption models.

The underestimate of the pion/quasielastic ratio in particular at higher energies could be due to, among other possibilities, an underestimate of the pion production cross section or an overestimate of the CCQE-like cross section. Both, which means for the latter the fake CCQE events, depend directly on the input at the nucleon level, i.e., in particular on the axial form factor C_5^A of the Δ resonance (see Ref. [1] for details). In the above calculations, we have used

$$\left[C_5^A(Q^2)\right]_I = C_5^A(0)\left[1+\frac{aQ^2}{b+Q^2}\right]\left(1+\frac{Q^2}{{M_A^I}^2}\right)^{-2}; \tag{1}$$

with $a=-0.25$, $b=0.04\ \mathrm{GeV}^2$, $M_A^I = 0.95$ GeV obtained from a fit to the ANL bubble chamber data and the PCAC value of $C_5^A(0) = 1.17$. However, the ANL and BNL results differ with the BNL result being approximately 30% higher. To account for the BNL findings, we introduce — following Ref. [5] — a dipole form factor

$$\left[C_5^A(Q^2)\right]_{II} = C_5^A(0)\left(1+\frac{Q^2}{{M_A^{II}}^2}\right)^{-2}, \tag{2}$$

with $M_A^{II} = 0.94$ GeV. The results for both parametrizations are shown in Fig. 4 and Fig. 5 together with the data of ANL and BNL. The shape of the BNL distribution is described well by both form factors (right panel of Fig. 4) while the ANL data are overestimated by the dipole form. Still one should bear in mind that there is a small non-resonant background [6] that has been neglected in this channel. For a discussion of possible Deuterium effects, in particular at low Q^2, see Refs. [5, 7].

In the right panel of Fig. 3 we present our results for the single-π^+/QE ratio using the dipole form factor. We find a slight enhancement of the ratio but still underestimate the data. Note that the enhancement is much more moderate than in Fig. 5. This is due to the fact, that both, numerator and denominator, i.e., also the CCQE-like cross section, are increased when the dipole form factor is used and, as a consequence, the larger CCQE-like cross section compensates the enhancement in the pion cross section. From this comparison we conclude that an increase of the total pion production cross section on the nucleon compatible with the BNL data seems to be insufficient to describe this ratio at all energies. A similar result for the ratio has been recently obtained by Athar *et al.* [11].

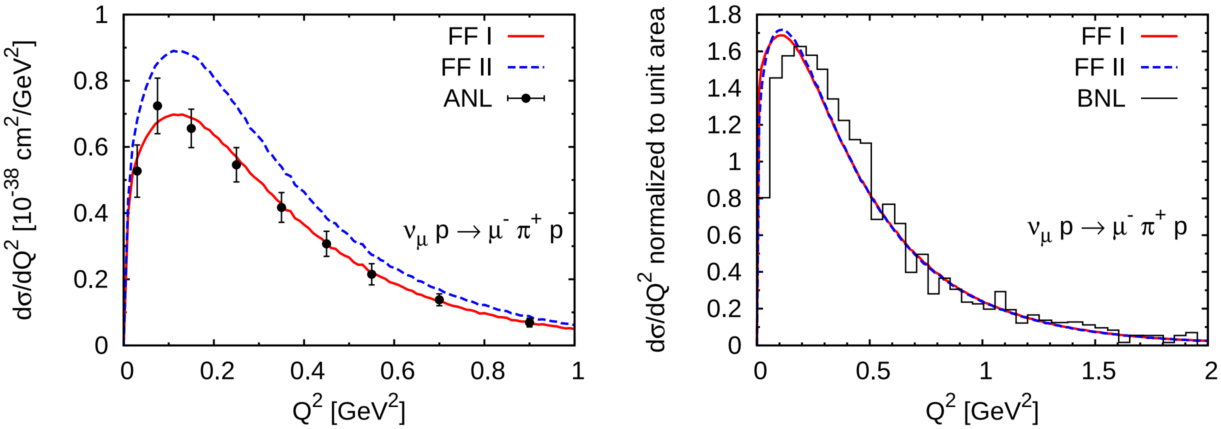

FIGURE 4. Differential cross section $\mathrm{d}\sigma/\mathrm{d}Q^2$ averaged over the ANL flux (left panel) and the BNL flux (right panel) [invariant mass cut at $W < 1.4$ GeV]. The data are taken from Refs. [8, 9]. The form factors are detailed in the text.

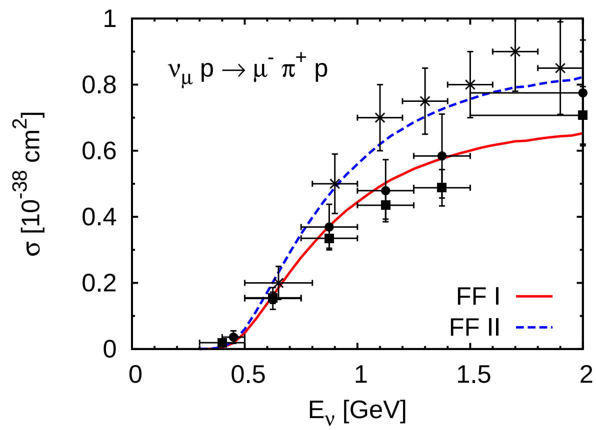

FIGURE 5. Total CC pion production cross sections compared to the pion production data of ANL [Refs. [10] (•), [8] (■)] and BNL [[9] (×)] The solid line has been obtained with $\left[C_5^A(Q^2)\right]_I$ while $\left[C_5^A(Q^2)\right]_{II}$ was used for the dashed line.

NC1π^0

In the left panel of Fig. 6, we show our results for NC single-π^0 production off ^{12}C as a function of the pion kinetic energy. We have averaged over the MiniBooNE energy flux which peaks at about 0.7 GeV neutrino energy [12]. In NC reactions the total pion yield is dominated by π^0 production, while π^+ dominate in CC processes (for details, see Ref. [13] and references therein). Comparing the dashed with the solid line (results without FSI and spectral function vs. full calculation), one finds a considerably change. The shape is caused by the energy dependence of the pion absorption and rescattering cross sections. Pions are mainly absorbed via the Δ resonance, i.e, through $\pi N \rightarrow \Delta$ followed by $\Delta N \rightarrow NN$. This explains the reduction in the region around $T_\pi = 0.1 - 0.3$ GeV. Pion elastic scattering $\pi N \rightarrow \pi N$ reshuffles the pions to lower momenta and leads also to charge exchange scattering into the charged pion channels. The vast majority of the pions comes from initial Δ excitation (dash-dotted line), their production in the rescattering of nucleons is not significant at these energies.

The right panel of Fig. 6 shows the results for NC single-π^0 production off ^{16}O averaged over the K2K energy flux which peaks at about 1.2 GeV neutrino energy [14]. Compared to the left panel, the spectrum is broader and extends to larger T_π due to the higher neutrino energy. The reduction in the region around $T_\pi = 0.1 - 0.3$ GeV is mainly caused by the pion absorption via the Δ resonance (compare dashed and solid lines). Again, pion production through initial QE scattering is not sizable.

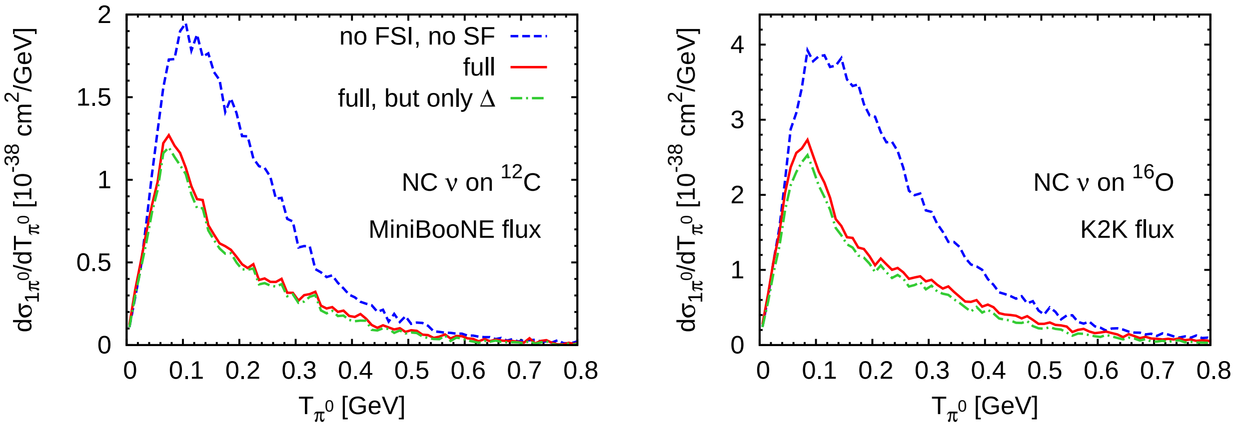

FIGURE 6. Left panel: NC induced single-π^0 production on ^{12}C as a function of the pion kinetic energy averaged over the MiniBooNE flux. The results were obtained with $\left[C_5^A(Q^2)\right]_I$. Right panel: same on ^{16}O averaged over the K2K flux. The dashed lines show our calculation without FSI or spectral functions, both included in the full calculation denoted with the solid lines. The dash-dotted lines indicate the contribution from the Δ resonance to the full calculation.

FINAL REMARK

Overall, the impact of FSI on observables is dramatic and not at all negligible. A qualitatively and quantitatively correct treatment is thus of great importance. More model-independent data are certainly needed.

ACKNOWLEDGMENTS

We thank O. Lalakulich for fruitful discussions. This work has been supported by the Deutsche Forschungsgemeinschaft.

REFERENCES

1. T. Leitner, O. Buss, L. Alvarez-Ruso and U. Mosel, Phys. Rev. C **79**, 034601 (2009), arXiv:0812.0587.
2. GiBUU Website, `http://gibuu.physik.uni-giessen.de/GiBUU`.
3. T. Katori, Measurement of muon neutrino charged current quasielastic (CCQE) double differential cross section in MiniBooNE, talk given at NUINT 09, May 17-22, 2009, Sitges, Spain, available online at `http://nuint09.ifae.es/Agenda.html`.
4. MiniBooNE, A. A. Aguilar-Arevalo *et al.*, arXiv:0904.3159.
5. K. M. Graczyk, D. Kielczewska and J. T. Sobczyk, arXiv:0907.1886.
6. E. Hernandez, J. Nieves and M. Valverde, Phys. Rev. D **76**, 033005 (2007), arXiv:hep-ph/0701149.
7. L. Alvarez-Ruso, S. K. Singh and M. J. Vicente Vacas, Phys. Rev. C **59**, 3386 (1999), arXiv:nucl-th/9804007.
8. G. M. Radecky *et al.*, Phys. Rev. D **25**, 1161 (1982).
9. T. Kitagaki *et al.*, Phys. Rev. D **34**, 2554 (1986).
10. S. J. Barish *et al.*, Phys. Rev. D **19**, 2521 (1979).
11. M. S. Athar, S. Chauhan and S. K. Singh, arXiv:0908.1442.
12. MiniBooNE, A. A. Aguilar-Arevalo *et al.*, arXiv:0806.1449.
13. T. Leitner, O. Buss, U. Mosel and L. Alvarez-Ruso, Phys. Rev. C **79**, 038501 (2009), arXiv:0812.1787.
14. K2K, S. Nakayama *et al.*, Phys. Lett. B **619**, 255 (2005), arXiv:hep-ex/0408134.